Published in final edited form as:
J Mech Behav Biomed Mater. 2013 October ; 26: 43–53. doi:10.1016/j.jmbbm.2013.05.021.

Bioerodible Calcium Sulfate/Poly(β-amino ester) Hydrogel Composites

Bryan R. Orellana[a], **Mark V. Thomas**[b], **Thomas D. Dziubla**[c], **Nihar M. Shah**[c], **James Z. Hilt**[c], and **David A. Puleo**[a,*]

[a]Center for Biomedical Engineering, Wenner-Gren Research Lab, University of Kentucky, Lexington, KY 40506-0070, USA

[b]College of Dentistry, University of Kentucky, Lexington, KY 40536-0297, USA

[c]Department of Chemical and Materials Engineering, University of Kentucky, Lexington, KY 40506-0046, USA

Abstract

The capacity to quickly regenerate or augment bone lost as a result of resorption is crucial to ensure suitable application of prosthetics for restoring masticatory function. Calcium sulfate hemihydrate (CS)-based bone graft substitute composites containing poly(β-amino ester) (PBAE) biodegradable hydrogel particles were developed to act as a 'tenting' barrier to soft tissue infiltration, potentially providing adequate space to enable vertical bone regeneration. CS has long been recognized as an osteoconductive biomaterial with an excellent reputation as a biocompatible substance. Composite samples were fabricated with varying amounts (1 or 10 wt%) and sizes (53–150 or 150–250 μm) of gel particles embedded in CS. The swelling and degradation rates of PBAE gels alone were rapid, resulting in complete degradation in less than 24 hours, an important characteristic to aid in controlled release of drug. MicroCT images revealed a homogeneous distribution of gel particles within the CS matrix. All CS samples degraded via surface erosion, with the amount of gel particles (*i.e.*, 10 wt% gel particles) having only a small, but significant, effect on the dissolution rate (4% vs. 5% per day). Compression testing determined that the amount, but not the size, of gel particles had a significant effect on the overall strength of the composites. As much as a 75% drop in strength was seen with a 10 wt% loading of particles. A pilot study using PBAE particles loaded with the multipotential drug curcumin demonstrated sustained release of drug from CS composites. By adjusting the amount and/or size of the biodegradable gel particles embedded in CS, mechanical strength and degradation rates of the composites, as well as the drug release kinetics, can be tuned to provide sufficient, multi-functional 'space-making' bone grafting substitutes.

1. Introduction

Dental implants have become a preferred method for replacing teeth lost to trauma or disease. Unfortunately, the disease processes that result in tooth loss may also cause the loss of supporting bone (Shimazu et al., 2006). Implant placement requires sufficient bone to

*To whom correspondence should be addressed: David Puleo, Ph.D., 209 Wenner-Gren Lab, Center for Biomedical Engineering, University of Kentucky, Lexington, KY 40506-0070, USA, Tel: +1-859-257-2405, Fax: +1-859-257-1856, puleo@uky.edu.

allow a proper anchor (Choi et al., 2004; Shimazu et al., 2006). Thus, bone regeneration or augmentation is often needed prior to or concomitant with implant placement (Choi et al., 2004; Shimazu et al., 2006). Guided bone regeneration (GBR) is a common technique in which a barrier membrane is used to create a protected 'healing chamber' where bone growth may occur. The barrier helps stabilize the blood clot and graft material and helps exclude the ingrowth of epithelium or fibrous connective tissue, either of which may interfere with the more slowly growing immature bone tissue (Simion et al., 2007). These membranes may be either resorbable (*e.g.*, collagen) or nonresorbable (*e.g.*, expanded polytetrafluoroethylene), although a second surgery is needed to remove the latter.

GBR membranes are often used in conjunction with an autogenous bone graft because of their tendency to collapse and subsequent inability to create the growth space by themselves (Donos et al., 2002; Hitti and Kerns, 2011). Although autogenous bone has been widely accepted as the gold standard augmentation material, its availability from intra-oral donor sites is limited (Choi et al., 2004; Strietzel et al., 2007; Tamimi et al., 2009). In the oral cavity, donor tissue is often harvested from the ramus or symphysis of the mandible, and this can lead to undesirable donor site morbidity (Chiapasco, 2009; Chiapasco et al., 2007; Clavero and Lundgren, 2003; Gao et al., 2007; Guarnieri et al., 2006; Hitti and Kerns, 2011; Jamali et al., 2002; Kenley et al., 1993; Kenny and Buggy, 2003; Lewis et al., 2006; Tay et al., 1999; Triplett and Schow, 1996). A biologically compatible, synthetic bone grafting substitute that is osteogenic, biodegradable/bioerodible, and provides spacing-making functionality could help eliminate the need for harvested bone or GBR membranes in the future.

Researchers have investigated many biocompatible ceramic materials as scaffolds for bone regeneration in attempts to replace the gold standard use of autogenous bone grafts. Calcium phosphates, such as hydroxyapatite and tricalcium phosphate, have been given much attention because of their likeness to natural bone mineral (Ginebra et al., 2006; Handschel et al., 2002; Hesaraki et al., 2009; Jamali et al., 2002; Kenny and Buggy, 2003; Zhang and Zhang, 2002). Calcium sulfate (CS) hemihydrate has long been recognized as an osteoconductive biomaterial with an excellent reputation as a biocompatible substance (Guarnieri et al., 2004; Lewis et al., 2006; Pecora et al., 1997; Thomas and Puleo, 2009; Thomas et al., 2005). In fact, it was one of the first bone substitutes used in orthopedics and dentistry (Guarnieri et al., 2004). CS has been called upon for a variety of applications, such as craniofacial and long bone defects, as well as osseous cavities related to tumors and cysts (Jamali et al., 2002). Characteristically, it has similar mechanical strength to that of cancellous bone (Hak, 2007). *In vivo,* CS is well tolerated, having the unique ability to become osteogenic in the presence of bone and completely absorbed by the host without inducing a significant inflammatory response (Guarnieri et al., 2004; Lewis et al., 2006; Thomas and Puleo, 2009; Thomas et al., 2005).

In the present study, CS-based bone graft substitute composites with embedded poly(β-amino ester) (PBAE) biodegradable hydrogel particles were developed to act as a 'tenting' barrier to soft tissue infiltration, thereby potentially enabling vertical bone regeneration, ultimately leading to a suitable depth of bone for implantation of a prosthesis. The photocrosslinked biodegradable gel particles presented in this study are part of a family of materials initially developed by Anderson *et al.* (Anderson et al., 2006; Hawkins et al., 2009). These gels can have a wide range of physical/chemical properties based on their macromer formulations (Anderson et al., 2006). For the purpose of the composite system presented, a gel with a rapid degradation rate was selected as the filler that may also serve as a delivery vehicle for pharmaceutical agents. The introduction of drug-loaded biodegradable gel particles into the composite matrix could improve the osteogenic properties of CS through a tailored, controlled release of bioactive molecules. Being able to control the

delivery of drugs to a bony defect allows for tunable dosing, as well as for extended retention time of drugs being released (Yamamoto et al., 2003). The influence of composite composition on physical and chemical characteristics, namely mechanical strength and modulus, dissolution, and morphology, was studied. In addition, a pilot release study was conducted to demonstrate controlled release of the multipotential drug curcumin from PBAE particles embedded in a CS matrix.

2. Materials & Methods

2.1. PBAE gel Synthesis

A11 PBAE macromer was synthesized according to previously described methods (Anderson et al., 2006; Hawkins et al., 2009). In brief, step-growth polymerization was performed by combining a 1.4:1 molar ratio of diethylene glycol diacrylate (2.079 g; Polysciences, Inc., Warrington, PA) and 3-morpholinopropyl amine (1.0 g; Sigma Aldrich, St. Louis, MO). The reaction took place in a flask partially submerged in a silicon oil bath pre-heated to 85°C. After continuously stirring the reaction mixture for 16 h, it was removed from the heat and stored at 4°C until used.

Biodegradable hydrogels (HG) were subsequently made using a photoinitiated polymerization process. Two grams of cooled macromer were combined with 1 wt% of 2,2-dimethoxy-2-phenyl-acetophenone (DMPA; Sigma Aldrich) initiator and dissolved in 1.25 mL of dimethylsulfoxide. After vortexing for 60 sec, the homogeneous mixture was sandwiched between two glass plates separated by a 1.5 mm Teflon spacer. The macromer was exposed to UV radiation using a Lesco UV flood source (14 mW/cm^2) for 5 min to initiate and propagate the photopolymerization process. After polymerization, the gel was removed from the glass, washed for 30 min in ethanol to remove any unreacted initiator and macromer, and then freeze-dried.

2.2. PBAE Swelling and Degradation

Swelling was measured as reported by Hawkins *et al.* (Hawkins et al., 2011). Square (1 cm^2) HG samples were submerged in deionized (DI) water or PBS and incubated at 37°C. For the first hour, samples were removed from the fluid, carefully dabbed dry, weighed, and placed back into fluid every 10 min. During the second and third hours, samples were removed and weighed in the same fashion every 20 min. After three hours, the time intervals were increased to every hour until the sample could no longer be handled or the samples were completely degraded. The extent of swelling [S%] was determined using, equation 1

$$S\% = \frac{M_t - M_o}{M_o} \times 100 \quad \text{[Eq. 1]}$$

where M_t was the mass at a particular time point and M_o was the initial mass.

2.3. Composite Formation

The composites consisted of calcium sulfate hemihydrate (Sigma Aldrich) as the structural matrix and varying amounts of A11 HG particles. Gel particles were hand-ground from polymerized gel slabs. In order to coat the gel particles and prevent them from sticking to one another, as well as to allow grinding to be efficient, small amounts of CS powder were added during grinding. Particle sizes of 53–150 μm and 150–250 μm were obtained by grinding and sieving. To make control (HG-free) samples, 1 g of CS powder was mixed with 800 μL of DI water in a 3 ml non-sterile syringe for about 30 sec. The slurry was injected into a custom-fabricated Delrin mold that could yield up to 46 samples with an average diameter of 4.75 mm and a height of 6.5 mm. Although cylindrical samples were made for

the present studies, this injection method allows for the fabrication of nearly any shape, including complex geometries. The mold was placed in a 43°C oven for 24 h to set the CS. For 1 wt% HG composite samples, 0.01 g HG was mixed with 0.98 g CS and 850 μL DI water; samples with 10 wt% HG consisted of 0.1 g HG, 0.8 g CS, and 900 μL DI water. As with the controls, the composite mixtures were loaded into the mold and set at 43°C for 24 h.

2.4. PBAE Particles and Composite Microarchitecture

2.4.1. PBAE Microarchitecture—Using an Olympus IX51 light microscope, a small amount of PBAE gel particles from each size fraction, 53–150 and 150–250μm, were placed on a glass slide and visually assessed. The physical structure of the particles was investigated to develop a qualitative understanding of their size distribution for a particular sieved fraction, as well as their appearance when embedded in a CS matrix. In addition to qualitative observations, particle size was quantified using ImageJ.

2.4.2. Composite Microarchitecture—To monitor the distribution of HG particles within the CS matrix, microcomputed tomography (microCT) was used. Using a Scanco Medical μCT-40 scanner, specimens were evaluated with standard resolution having 250 projections with 1024 samples each. Additional parameters were set as follows: 92 μm increments, 0° angle, 70 kVp, 114 μA, 0.5 mm Al filter, and a voxel size of 12 μm. The resulting microarchitectural images were qualitatively investigated for any particle distribution trends. To qualitatively and quantitatively assess the composites, samples were evaluated with a lower threshold level of 109 before running a built-in ‘bone trabecular morphometry’ analytical tool. This tool created a three-dimensional reconstruction that allowed assessment of the composite structure and its embedded gel particles as well as provided the volume percentage of embedded gel particles, average particle size, and average spacing between particles.

2.5. Composite Erosion

Destructive mass loss testing was performed to monitor erosion of the composites. Samples of each type (control, 1 wt% HG, and 10 wt% HG) were weighed, measured (height and diameter), placed in separate plastic vials containing 4 mL of phosphate-buffered saline (PBS), pH 7.4, and incubated on a plate shaker at 37°C. Every four days, samples were removed and dried in a 43°C oven for a minimum of 24 hrs. For the remaining samples, the PBS in vials was replaced with fresh PBS. The dried samples were weighed to determine the amount of mass lost.

2.5.1. Degradation: Changes in Fluid Volume—Mass loss using different fluid volumes was tested to determine the effects on composite dissolution rates. The experimental method for mass loss described in section 2.5 was used. Five different fluid volumes were tested: 0.5, 1.5, 3, 4, and 6 mL.

2.6. Composite Mechanical Testing

Compression testing was performed using a Bose ELF 3300 system. Samples without any noticeable external defects, such as cracks or voids, were chosen for testing. With the present fabrication process, more than 80% of the samples were suitable. Contact surfaces were lightly sanded, if necessary, using 600 grit SiC paper to provide smooth, parallel surfaces in contact with the compression platens. Control, 1 wt% HG, and 10 wt% HG samples were tested at a rate of 0.5 N/sec until failure. Compressive modulus (M) and ultimate compressive strength (UCS) were calculated.

2.7. Pilot Release Study with Curcumin

A pilot study of drug delivery from the composites was performed to demonstrate the potential for controlled release. PBAE gels were produced with 50 wt% curcumin using a method previously reported (Wattamwar et al., 2012). This method allows for complete control of drug loading into the gel system to help achieve potentially therapeutic amounts. After synthesis, finished gels were thoroughly washed with acetonitrile to remove unreacted components (macromere, initiator, and drug) and then lyophilized overnight. As for drug-free PBAE, gels were hand-ground with small amounts of CS and sieved to obtain particles ranging from 53–150 μm or 150–250 μm. Drug-loaded particles were washed with DI water for 1 minute to remove CS before being filtered and lyophilized once more. Composites were produced using the same steps described in section 2.3 for both 1 and 10 wt% HG composite formation.

Loaded composite and blank CS control samples were weighed, submerged in 4 mL of PBS, and placed on a plate shaker in a 37°C incubator. To maintain sink conditions, supernatant was collected and fresh PBS was added every 4 days as conducted for the mass loss studies. This continued until all samples completely degraded. For each measurement, 1 mL of collected supernatant was treated with 50% ethanol to dissolve any suspended drug and filtered (0.45 μm). Absorbance of gel washings and treated supernatants was measured at 420 nm, with concentrations determined by comparison to curcumin standards.

2.8. Statistics

Statistical analysis of the results was performed using either a two-tailed, unpaired t-test or two-way ANOVA. As appropriate, this was followed with a Tukey-Kramer multiple comparisons post hoc test. Differences between groups were considered to be significant with p-values <0.05.

3. Results

3.1. PBAE Swelling and Degradation

The degree of hydrogel swelling and degradation based on the mass of liquid absorbed by the samples is displayed in Figure 1. During the first 60–80 minutes, the gels swelled quickly, but the rate gradually slowed and reached a plateau around 160 minutes. After this initial stage, the full extent of swelling appeared to reach a maximum for gels submerged in PBS, and the samples did not show any significant signs of further swelling. After 300 minutes, the gels submerged in DI water began to absorb liquid again at a significantly higher rate ($p<0.0001$) that continued until the end of the experiment. The study was concluded around 420 minutes when the samples became fragile and difficult to handle.

3.2. Composite Microarchitecture

3.2.1. Qualitative Evaluation—Under a light microscope, gel particles were seen as large, irregularly shaped objects along with some dispersed prism-like particles considered to be residual CS used during grinding (Figure 2). Quantitative analysis showed that the size distribution of gel particles was within the expected limits, 53–150 μm and 150–250 μm (data not shown).

MicroCT analysis showed the size and distribution of gel particles embedded in CS (Figure 3). In samples with 10 wt% loading of particles, there was a homogeneous distribution of particles throughout the CS matrix (Figures 3D, E). Composites with 1 wt% loading of gel particles showed a more sparse distribution, but the particles still appeared homogeneously distributed throughout the matrix (Figures 3B, C). Even though composites showed a good distribution of particles, they were not without some minor defects. For example, samples

had a small air pocket defects (black arrows in Figure 3) embedded along with gel particles. These defects were nearly spherical in nature and thus easily distinguishable from gel particles, which had irregular shapes as previously shown in Figure 2.

3.2.2. Quantitative Evaluation—Quantitative analysis was performed to develop a greater understanding of the physical structure of the composites than could be achieved by a qualitative analysis alone. Figure 4 shows the porosity, spacing between particles/voids, and particle/void size for the different composite compositions. The porosity of about 8.31% for 10 wt% HG (150–250 μm) loading was significantly different ($p<0.001$) from all other loadings tested (Figure 4A). For all other configurations, there were no significant differences in porosity among them.

For the spacing between particles/voids, the blank samples were significantly different ($p<0.001$) compared to 1 wt% HG (53–150 μm), 10 wt% HG (53–150 μm), and 10 wt% HG (150–250 μm) samples (Figure 4B). Differences in void spacing between the 1 wt% HG loadings for both particles sizes was significantly different [$p<0.01$, 1 wt% HG (53–150μm) vs. 1 wt% HG (150–250μm)]. When comparing the different loadings for a particular particle size, the distance between particles for the 1 wt% HG loadings was significantly larger ($p<0.001$) compared to that for 10 wt% HG loadings, except for the 1 wt% HG (53–150μm) vs. 10 wt% HG (53–150μm) relationship, which was significantly different with a $p<0.05$.

The particle and/or void size (Figure 4C) demonstrated significant differences for 1 wt% HG (53–150 μm) versus both 10 wt% HG (53–150 μm) ($p<0.001$) and 10 wt% HG (150–250 μm) ($p<0.05$).

3.3. Composite Degradation

All sample groups were tested simultaneously during the mass loss experiments. Loading 1 wt% of gel particles did not have a significant effect on the dissolution rate (-3.71%/day) of the overall composite (Figure 5). Increasing the loading to 10 wt%, however, significantly increased the dissolution rate to −4.42%/day ($p<0.05$), even though complete dissolution varied by only about four days.

3.3.1. Degradation: Changes in Fluid Volume—Similar to the composite degradation experiment, all sample types were tested using the same PBS to avoid fluid-dependent effects on dissolution except volume change. Shown in Figure 6, small fluid volumes of 0.5 or 1.5 mL led to significantly slower dissolution, −0.6 or −2.7%/day, respectively ($p<0.001$). Increasing the fluid volumes to 3, 4, or 6 mL contributed to dissolution rates of −5.1, −6, or −6.6%/day, respectively. When compared to 3 mL, fluid volumes of 4 mL and 6 mL caused significantly faster dissolution rates ($p<0.05$ and $p<0.001$, respectively).

3.4. Composite Mechanical Testing

Effects of HG loading on the compressive mechanical properties are shown in Figure 7. The ultimate strength for blank CS samples was significantly greater than that of both 10 wt% HG ($p<0.0001$) and 1 wt% HG loadings ($p<0.001$). Elastic modulus of blank CS, however, was only significantly greater than that of the 10 wt% HG loadings ($p<0.0001$). Composite samples with 1 wt% HG had 80–90% of the control strength, and 1 wt% addition of gel particles had no significant effect on the modulus when compared to blank samples. Adding 10 wt% HG resulted in 40–50% of the ultimate strength and 25–30% of the modulus of particle-free samples. Comparing samples loaded with 1 wt% HG of either 53–150 μm or 150–250 μm particles showed a significant difference ($p<0.01$) in their strength (3.99 ± 1.19 MPa versus 4.89 ± 0.38 MPa, respectively), however, there was no significant difference in

the elastic modulus (401.35 ± 156.92 MPa and 369.1 ± 224.58 MPa, respectively). The strength of 10 wt% HG composites for both particle sizes was also significantly different [$p<0.01$; 2.57 ± 0.24 MPa (53–150 μm) and 1.94 ± 0.36 MPa (150–250 μm)], but the difference between their elastic moduli was not significant. Comparing the two different particle sizes and their different weight percentages, there were significant differences as well. For either particle size, the ultimate strength of composites containing 1 wt% HG particles was significantly greater than that for 10 wt% HG loadings [$p<0.05$ for 1 wt% HG (53–150μm) vs. 10 wt% HG (53–150μm); $p<0.0001$ for all other composite comparisons]. The elastic modulus of 1 wt% HG (53–150 μm) vs. both 10 wt% HG loadings was significantly different ($p<0.001$), as were the differences in modulus between 1 wt% HG (150–250 μm) and both 10 wt% HG loadings ($p<0.01$).

3.5. Drug (Curcumin) Release

Figure 8 illustrates the release kinetics from a pilot study of CS composites containing PBAE particles loaded with curcumin. For both 1 wt% HG loadings, release of curcumin was steady, where about 30% was appeared during the first 4 days and only 60–70% of the drug was released during the first half (14 days) of the study. Over the course of the study, there was a slow decay of the daily release percentage from the 1 wt% HG composites: 8%/day at 4 days, 6%/day at 10 days, and 4%/day at 20 days. Conversely, 10 wt% HG loadings started with a larger burst (50–60%) release of drug over the first 4 days followed by nearly 90% of the loaded drug being released during the first 14 days of the four week study.

4. Discussion

The aim of the present studies was to understand the physical and chemical characteristics of a composite bone graft substitute that has the potential to act as a ‘tenting’ barrier to soft tissue infiltration for creating a chamber for bone regeneration, while simultaneously allowing for the controlled release of bioactive agents. The regenerated bone could provide a sufficient platform for stable placement of dental implants in periodontal applications.

4.1. PBAE Swelling and Degradation

Degradable PBAE gel particles were synthesized to serve as a protective delivery vehicle for osteogenic agents and/or other drug(s) when embedded in a CS matrix. Initial studies were performed to determine whether swelling of the particles following exposure to a physiological environment would be extensive enough to adversely affect the overall composite structure. *In vitro* experiments showed three distinct stages in the swelling profiles. After the initial swelling stage, absorption of liquid slowed, eventually reaching a plateau. It has been well established that swelling of hydrogel occurs due to the electrostatic repulsion of ionic charges within the polymer due to the presence of absorbing liquid (Karadağ and Saraydın, 2002; Zhou et al., 1996). During the plateau phase, osmotic forces driving fluid into the hydrophilic gels equaled the opposing elastic force created by the stretching of the crosslinked polymer. After the plateau, the polymer backbone began failing at a faster rate through hydrolytic scission of the ester bonds, yielding small molecule bis(β-amino acids), diol products, and poly(acrylic acid) kinetic chains (Anderson et al., 2006). This gradual breakdown of the polymer matrix allowed for further expansion of the mesh and continued absorption of liquid into the gel. Anderson *et al.* previously demonstrated that A11 PBAE gels degrade very rapidly (<24 hrs), which is similar to the results seen in the present study where gels began to rapidly break down through hydrolysis, beginning around 4–5 hrs, and resulted in complete degradation within 24 hrs (Anderson et al., 2006).

An advantage of the PBAE family of hydrogels is that there are a variety of possible combinations of diacrylates and amines that can produce a similar range of properties.

Hawkins *et al.* studied a PBAE comprising poly(ethylene glycol) diacrylate (H) and isobutylamine (6) in a 1.2 molar ratio (Hawkins et al., 2011). The components were different from those used for the present A11 gels, however, the H6 system also degraded in less than 24 hours. Although the H6 gel swelled about 50% more during the first 4 hrs compared to the A11 gels, they both reached a plateau followed by a rapid degradation of the polymer starting around 4–5 hrs (Hawkins et al., 2011). The similarities between these two PBAEs demonstrate the versatility of this gel family and how the gel particles in the CS/HG composite system may be altered to accommodate different formulations as needed.

4.2. Composite Morphology

When creating particles to be embedded in CS, gel slabs were ground with a small amount of calcium sulfate to act as a 'drying agent' similar to talcum powder to prevent particles from sticking to one another. The harder CS also served as an abrasive to enhance efficiency of grinding. Images showed a CS crystals remaining with the gel particles after sieving. The smaller 53–150 μm gel particles had more residual calcium sulfate compared to the larger 150–250 μm particles. Calcium sulfate is inherently more dense than the gels. Therefore, the greater amount of CS present with the 53–150 μm size particles must be taken into account in future studies investigating drug loading and release. The larger particles have a smaller surface area to volume ratio compared to the smaller particles, thus requiring a smaller amount of CS to coat and process the particles.

Qualitative analysis of microCT images indicated a homogeneous distribution of gel particles at both 1 and 10 wt% loadings. The composite slurry, when mixed well, allows for a short working window for easy filling of the molds because of the rapid setting nature of CS. Due to the viscosity of this slurry, gel particles were suspended and prevented from aggregating with one another. Also, any buoyancy effects that could cause particles to collect at one end of the sample and thereby lead to inhomogeneity were prevented. Once set, the gel particles were locked in place, and any swelling of particles that may have occurred while mixing the slurry was reversed resulting in contraction of these particles. Overall, protective voids were created in which dried gel particles reside. An important feature of this process was the creation of a tolerance 'gap' between the wall of the voids and the HG particles preventing composite failure due to swelling of gel particles during CS dissolution. In addition, because the irregularly shaped voids are stress concentrators themselves, they may also affect structural integrity under an applied load.

Quantitative evaluation of the composites' porosity showed a dramatic decrease for the 10 wt% HG loading of 53–150 μm particles (2.67%) compared to the 10 wt% HG of 150–250 μm particles (8.31%). The presence of residual CS, especially with the 53–150 μm size fraction, could affect loading because the CS will incorporate with the rest of the matrix, leaving behind a smaller quantity of gel particles. Interestingly, residual CS did not play a significant role when comparing the 1 wt% HG loadings for both particle sizes. The contribution of air pockets to the porosity, particle/void spacing, and size calculations for 1 wt% HG specimens may have counteracted the effects of residual CS described above. However, the number of air pockets within the 10 wt% HG composites may not have contributed significantly to these void fraction due to the much larger quantity of gel particles present. This trend is exemplified by the particle size measurements for 1 wt% HG (53–150 μm) and 10 wt% HG (53–150 μm), where the resulting porosity values were significantly different, although the particles used for these composites were the same.

4.3. Composite Degradation

CS composites degrade by means of dissolution and subsequent surface erosion. Bulk degradation was not observed because of the dense nature of the ceramic and lack of an

open-celled porous network. Although the gel particles created a porous structure within the matrix, the pores were 'closed'. This structure should enable the composites to approach zero-order kinetics, whereby only the gel particles exposed on the surface during CS erosion will be permitted to swell, degrade, and release their active molecules. The HG loading-independence of composite degradation rate may allow for easy tuning to provide long enough mechanical stability or protection from soft tissue infiltration while also allowing the sustained delivery of a sufficient amount of drug-loaded HG particles to stimulate bone formation.

Lewis *et al.* investigated a CS composite containing carboxymethylcellulose (CMC) or hyaluronan (HY) to improve handling or workability, mechanical, and degradation properties (Lewis et al., 2006). They showed that the introduction of these biopolymers allowed for better handling properties as well as increased compressive strength. Introduction of CMC and HY, however, had a drastic effect on the degradation rate of the composite. As the mass of CMC increased, the degradation rate also increased (12%/day for a loading of 10% CMC compared to 1.6%/day for plain CS) (Lewis et al., 2006). For the current study, addition of 1 wt% PBAE particles did not have a significant effect on the dissolution rate of CS (3.71%/day), and after increasing the amount of particles to 10 wt%, the rate of dissolution increased to 4.42%/day. Gao *et al.* reported similar erosion rates (4.3%/day to 5.2%/day) for CS and CS/gelatin composites (Gao et al., 2007). Incorporation of calcium phosphate (CaP) microspheres within a CS matrix increased the retention time of the composite compared to blank CS, prolonging the absorption of CS *in vivo* (Urban et al., 2007). Urban *et al.* were also able to demonstrate a greater amount of bone formation over the course of 26 weeks in response to the CS/CaP composite compared with the CS pellets alone (Urban et al., 2007). In the present study, the dissolution rate of CS was not compromised by the incorporation of HG particles. Using the original dissolution rate for CS, the embedded PBAE particles could serve as delivery vehicles for bioactive drugs.

4.3.1. Fluid Volume Effects—The volume of fluid present during composite degradation *in vivo* is unknown, yet the rate of fluid turnover is likely to have a notable effect on the rate of degradation. A degradation study utilizing multiple fluid volumes was performed to simulate the effects of different sink (or non-sink) conditions that would result from different fluid volumes and/or turnover rates. The idea behind this experiment was to show the diversity of dissolution rates based on the volume of fluid possibly present in a particular wound site. In the case of implanting a CS composite *in vivo*, the rate at which the implant erodes will be key for proper resorption and replacement with new tissue. As would be expected, smaller fluid volumes of 0.5 or 1.5 mL significantly reduced the rate of dissolution, 0.6%/day or 2.7%/day, respectively. Conversely, increasing the fluid volume above 4 mL increased the rate of dissolution to about 6%/day. The similarity of the faster dissolution rates (6%/day and 6.6%/day) for fluid volumes ≥4 mL suggested a threshold for the sink conditions was reached that caused dissolution to become constant. Considering the surface area of the sample versus the volume of fluid used, it is fair to conclude that dissolution of cylindrical calcium sulfate samples with an estimated surface area of 114 mm^2 (assuming sample diameter of 4.66 mm and height of 6.7 mm) will be constant regardless of the volume used above the 3–4 mL threshold because of the limited amount of surface exposed.

4.4. Composite Mechanical Properties

Mechanical stability is important when developing a bone graft substitute material that will provide support for bone formation. Depending on the procedure performed, the majority of the graft could reside within a defect site where surrounding bony tissue would act as a protective shelter. The remaining portion, or cap, would protrude from the defect to provide

both an aid for the vertical augmentation of bone and act as a 'tenting apparatus' distributing any load from overlying soft tissue. An example of such a space-making site is the socket remaining after removal of a tooth. A graft placed into such a site (or a blood clot which fills the socket) will be protected and stabilized by the surrounding bony walls.

A more challenging application would be sites that are not 'space-making', *i.e.*, sites that lack topography to contain and protect the 'regeneration chamber'. This would require development of implant materials that are strong enough to create and maintain space in the absence of any surrounding bone, as well as prevent soft tissue ingrowth to permit new bone formation. The best example would be vertical bone growth in a badly resorbed mandible or maxilla.

Gel loading of 1 wt% had a 10–20% decrease in the mechanical strength of the CS/HG composites. Because the 1 wt% HG loading ratio did not affect the dissolution rate, these composites may be preferable to blank CS in clinical applications because of the added potential as a drug delivery vehicle. Addition of 10 wt% HG decreased composite strength and modulus by 50–60% and 70–75%, respectively, creating a much weaker material. Thus, 10 wt% HG may represent an upper threshold for particle loading because of the adverse effects on mechanical integrity. Any differences among the composite samples can be explained by differences in their microstructure, *e.g.*, stress concentrators formed by voids housing gel particles, minor microstructural defects, and growth and propagation of crystals as CS sets. Injectable calcium phosphate cements containing 0–15 wt% of hydroxyapatite had compressive strength ranging between 2.5 and 4.5 MPa (Kim and Jeon, 2012). Interestingly, these results are similar to the strengths measured in the present study. Blank CS, 1 wt%, and 10 wt% gel samples resulted in compressive stresses of 5.5, 4, and 2 MPa, respectively.

Lewis *et al.* investigated CS/biopolymer composites (Lewis et al., 2006). Their blank CS samples had a 10 MPa compressive strength that was stronger than the present materials. An interesting aspect of CS/biopolymer composites compared to CS/HG was the similarity in volume of fluid used for production compared to the differences found in the resulting mechanical strengths. The liquid to powder ratio of Lewis *et al.* ranged between 0.8–1.33 mL/g compared to present 0.8–0.9 mL/g (Lewis et al., 2006). Another group investigated the use of an α-hemihydrate CS for a composite structure incorporating biomimetic apatite nanoparticles for controlled drug delivery (Hesaraki et al., 2009). That study utilized two liquid to powder ratios, 0.6 and 0.4 mL/g. Although these ratios were lower than those used in Lewis' or the present study, the compressive strength of CS (2–4 MPa) was comparable (Hesaraki et al., 2009). The similarities in compressive strength help demonstrate that the liquid to powder ratio does not appear to have a significant effect on the strength of the material within the ranges presented. An attempt to optimize liquid content and/or loading of gel particles to achieve a desired grafting device will be pursued in the future.

4.5. Drug (Curcumin) Release

As a naturally occurring drug originating from the dietary spice turmeric, curcumin has a broad range of therapeutic functions, including anti-inflammatory, antioxidant, anti-bacterial, and more recently, anti-resorptive activities (Cho et al., 2012; Ozaki et al., 2000; Wattamwar et al., 2012). With respect to osteotropic effects, curcumin exerts an inhibitory effect of bone resorption via enhanced osteoclast apoptosis (Ozaki et al., 2000), and it stimulates osteoblast differentiation (Gu et al., 2012). Early exposure of a multi-functional drug controllably released from the proposed CS composites could enhance bioactivity of the materials.

A pilot study to demonstrate sustained release of a drug from CS composites was conducted by releasing curcumin from drug-loaded PBAE gel particles embedded within a CS matrix. Wattamwar *et al.* originally developed the curcumin HG system in which the antioxidant is directly incorporated into the macromer prior to polymerization to prevent premature diffusion of drug from the gel matrix prior to hydrolysis (Wattamwar et al., 2012). Release was sustained over a one month period from both 1 and 10 wt% CS/HG composites, although the higher loading resulted in a greater initial burst. Continuous dissolution of CS permitted only the PBAE particles that were exposed to the surface of the composite to degrade and thereby allow the drug to be released. Additionally, the total exposed surface area slowly decreased during dissolution, which in turn allowed a smaller volume of exposed particles to release the drug. This phenomenon explains the slow decay in the daily rate of release. Regardless, the present results demonstrate that release of curcumin from HG is controlled by the way gel particles are exposed during erosion of CS composites.

5. Conclusion

Calcium sulfate-based composites with embedded poly(β-amino ester) biodegradable gel particles were developed to potentially serve as a bone graft substitute for vertical bone regeneration. The gel particles are intended to provide delivery of bioactive molecules to enrich the bone augmentation process without physically compromising the capacity of the composite to be used as a grafting substitute. It was determined that the PBAE gel particles were homogeneously distributed within the CS matrix, and the embedded particles had minimal impact on the zero-order dissolution rate. However, a destructive *in vitro* dissolution study showed that fluid volume turnover had a large effect on the rate at which these composites erode. PBAE particles resulted in as much as a 75% drop in composite strength with a 10 wt% loading of particles. On the other hand, the dissolution rate was minimally affected with the increased loading of gel particles, and the composites are designed for local drug delivery to help enhance tissue regeneration. A pilot study of curcumin delivery from HG particles embedded within the composites demonstrated sustained release of the drug that was governed by degradation of PBAE during dissolution of CS over time. Further developments will investigate the capacity of the composite bone graft substitute to deliver a broad range of drugs and ability to tailor the composites on a case-by-case basis.

Acknowledgments

This research supported by the National Institutes of Health (DE019645), Kentucky NASA EPSCoR (NNX08BA13A), and the National Science Foundation (EPS-0814194).

References

Anderson DG, Tweedie CA, Hossain N, Navarro SM, Brey DM, Van VKJ, Langer R, Burdick JA. A combinatorial library of photocrosslinkable and degradable materials. Adv. Mater. (Weinheim, Ger.). 2006; 18:2614–2618.

Chiapasco M. Bone augmentation procedures in implant dentistry. Quintessence Pub. Co. 2009

Chiapasco M, Zaniboni M, Rimondini L. Autogenous onlay bone grafts vs. alveolar distraction osteogenesis for the correction of vertically deficient edentulous ridges: a 2–4-year prospective study on humans. Clinical Oral Implants Research. 2007; 18:432–440. [PubMed: 17501979]

Cho D-C, Kim K-T, Jeon Y, Sung J-K. A synergistic bone sparing effect of curcumin and alendronate in ovariectomized rat. Acta Neurochir. 2012; 154:2215–2223. [PubMed: 23053289]

Choi B-H, Lee S-HR, Huh J-Y, Han S-G. Use of the sandwich osteotomy plus an interpositional allograft for vertical augmentation of the alveolar ridge. J Craniomaxillofac Surg. 2004; 32:51–54. [PubMed: 14729051]

Clavero J, Lundgren S. Ramus or Chin Grafts for Maxillary Sinus Inlay and Local Onlay Augmentation: Comparison of Donor Site Morbidity and Complications. Clinical Implant Dentistry and Related Research. 2003; 5:154–160. [PubMed: 14575631]

Donos N, Kostopoulos L, Karring T. Alveolar ridge augmentation using a resorbable copolymer membrane and autogenous bone grafts. An experimental study in the rat. Clin Oral Implants Res. 2002; 13:203–213. [PubMed: 11952741]

Gao C, Huo S, Li X, You X, Zhang Y, Gao J. Characteristics of calcium sulfate/gelatin composite biomaterials for bone repair. J. Biomater. Sci. Polym. Ed. 2007; 18:799–824. [PubMed: 17688742]

Ginebra MP, Traykova T, Planell JA. Calcium phosphate cements as bone drug delivery systems: A review. Journal of Controlled Release. 2006; 113:102–110. [PubMed: 16740332]

Gu Q, Cai Y, Huang C, Shi Q, Yang H. Curcumin increases rat mesenchymal stem cell osteoblast differentiation but inhibits adipocyte differentiation. Pharmacognosy magazine. 2012; 8:202–208. [PubMed: 23060694]

Guarnieri R, Grassi R, Ripari M, Pecora G. Maxillary sinus augmentation using granular calcium sulfate (surgiplaster sinus): radiographic and histologic study at 2 years. Int J Periodontics Restorative Dent. 2006; 26:79–85. [PubMed: 16515099]

Guarnieri R, Pecora G, Fini M, Aldini NN, Giardino R, Orsini G, Piattelli A. Medical grade calcium sulfate hemihydrate in healing of human extraction sockets: clinical and histological observations at 3 months. J Periodontol. 2004; 75:902–908. [PubMed: 15295959]

Hak DJ. The Use of Osteoconductive Bone Graft Substitutes in Orthopaedic Trauma. Journal of the American Academy of Orthopaedic Surgeons. 2007; 15:525–536. [PubMed: 17761609]

Handschel J, Wiesmann HP, Stratmann U, Kleinheinz J, Meyer U, Joos U. TCP is hardly resorbed and not osteoconductive in a non-loading calvarial model. Biomaterials. 2002; 23:1689–1695. [PubMed: 11922472]

Hawkins AM, Puleo DA, Hilt JZ. Effect of macromer synthesis time on the properties of the resulting poly(β-amino ester) degradable hydrogel. J. Appl. Polym. Sci. 2011; 122:1420–1426.

Hawkins AM, Satarkar NS, Hilt JZ. Nanocomposite Degradable Hydrogels: Demonstration of Remote Controlled Degradation and Drug Release. Pharm. Res. 2009; 26:667–673. [PubMed: 19118411]

Hesaraki S, Moztarzadeh F, Nemati R, Nezafati N. Preparation and characterization of calcium sulfate–biomimetic apatite nanocomposites for controlled release of antibiotics. Journal of Biomedical Materials Research Part B: Applied Biomaterials. 2009; 91B:651–661.

Hitti RA, Kerns DG. Guided Bone Regeneration in the Oral Cavity: A Review. The Open Pathology Journal. 2011; 5:33–45.

Jamali A, Hilpert A, Debes J, Afshar P, Rahban S, Holmes R. Hydroxyapatite/Calcium Carbonate (HA/CC) vs. Plaster of Paris: A Histomorphometric and Radiographic Study in a Rabbit Tibial Defect Model. Calcified Tissue International. 2002; 71:172–178. [PubMed: 12200649]

Karadağ E, Saraydın D. Swelling studies of super water retainer acrylamide/crotonic acid hydrogels crosslinked by trimethylolpropane triacrylate and 1,4-butanediol dimethacrylate. Polymer Bulletin. 2002; 48:299–307.

Kenley RA, Yim K, Abrams J, Ron E, Turek T, Marden LJ, Hollinger JO. Biotechnology and Bone Graft Substitutes. Pharmaceutical Research. 1993; 10:1393–1401. [PubMed: 8272399]

Kenny SM, Buggy M. Bone cements and fillers: A review. Journal of Materials Science: Materials in Medicine. 2003; 14:923–938. [PubMed: 15348504]

Kim SY, Jeon SH. Setting properties, mechanical strength and in vivo evaluation of calcium phosphate-based bone cements. J. Ind. Eng. Chem. (Amsterdam, Neth.). 2012; 18:128–136.

Lewis KN, Thomas MV, Puleo DA. Mechanical and degradation behavior of polymer-calcium sulfate composites. J. Mater. Sci.: Mater. Med. 2006; 17:531–537. [PubMed: 16691351]

Ozaki K, Kawata Y, Amano S, Hanazawa S. Stimulatory effect of curcumin on osteoclast apoptosis. Biochemical Pharmacology. 2000; 59:1577–1581. [PubMed: 10799655]

Pecora G, Andreana S, Margarone JE 3rd, Covani U, Sottosanti JS. Bone regeneration with a calcium sulfate barrier. Oral Surg Oral Med Oral Pathol Oral Radiol Endod. 1997; 84:424–429. [PubMed: 9347509]

Shimazu C, Hara T, Kinuta Y, Moriya K, Maruo Y, Hanada S, Minagi S. Enhanced vertical alveolar bone augmentation by recombinant human bone morphogenetic protein-2 with a carrier in rats. J. Oral Rehabil. 2006; 33:609–618. [PubMed: 16856959]

Simion M, Fontana F, Rasperini G, Maiorana C. Vertical ridge augmentation by expanded-polytetrafluoroethylene membrane and a combination of intraoral autogenous bone graft and deproteinized anorganic bovine bone (Bio Oss). Clin Oral Implants Res. 2007; 18:620–629. [PubMed: 17877463]

Strietzel FP, Reichart PA, Graf H-L. Lateral alveolar ridge augmentation using a synthetic nano-crystalline hydroxyapatite bone substitution material (Ostim): preliminary clinical and histological results. Clin Oral Implants Res. 2007; 18:743–751. [PubMed: 17888015]

Tamimi F, Torres J, Gbureck U, Lopez-Cabarcos E, Bassett DC, Alkhraisat MH, Barralet JE. Craniofacial vertical bone augmentation: A comparison between 3D printed monolithic monetite blocks and autologous onlay grafts in the rabbit. Biomaterials. 2009; 30:6318–6326. [PubMed: 19695698]

Tay BK, Patel VV, Bradford DS. Calcium sulfate- and calcium phosphate-based bone substitutes. Mimicry of the mineral phase of bone. The Orthopedic clinics of North America. 1999; 30:615–623. [PubMed: 10471766]

Thomas MV, Puleo DA. Calcium sulfate: properties and clinical applications. J. Biomed. Mater. Res. Part B. 2009; 88B:597–610.

Thomas MV, Puleo DA, Al-Sabbagh M. Calcium sulfate: a review. J. Long-Term Eff. Med. Implants. 2005; 15:599–607. [PubMed: 16393128]

Triplett RG, Schow SR. Autologous bone grafts and endosseous implants: Complementary techniques. Journal of Oral and Maxillofacial Surgery. 1996; 54:486–494. [PubMed: 8600266]

Urban RM, Turner TM, Hall DJ, Inoue N, Gitelis S. Increased Bone Formation Using Calcium Sulfate-Calcium Phosphate Composite Graft. Clinical Orthopaedics and Related Research. 2007; 459:110–117. [PubMed: 17415007]

Wattamwar PP, Biswal D, Cochran DB, Lyvers AC, Eitel RE, Anderson KW, Hilt JZ, Dziubla TD. Synthesis and characterization of poly(antioxidant β-amino esters) for controlled release of polyphenolic antioxidants. Acta Biomaterialia. 2012; 8:2529–2537. [PubMed: 22426289]

Yamamoto M, Takahashi Y, Tabata Y. Controlled release by biodegradable hydrogels enhances the ectopic bone formation of bone morphogenetic protein. Biomaterials. 2003; 24:4375–4383. [PubMed: 12922150]

Zhang Y, Zhang M. Calcium phosphate/chitosan composite scaffolds for controlled in vitro antibiotic drug release. Journal of Biomedical Materials Research. 2002; 62:378–386. [PubMed: 12209923]

Zhou W-J, Yao K-J, Kurth MJ. Synthesis and swelling properties of the copolymer of acrylamide with anionic monomers. Journal of Applied Polymer Science. 1996; 62:911–915.

Highlights

- Calcium sulfate/poly(β-amino ester) bone graft substitutes were developed.
- Homogeneously mixed PBAE particles minimally affected composite dissolution.
- Loading of particles must be balanced against decreased mechanical properties.
- Sustained release of a multifunctional drug was demonstrated.
- Composite properties can be tuned to provide different ‘space-making’ functions.

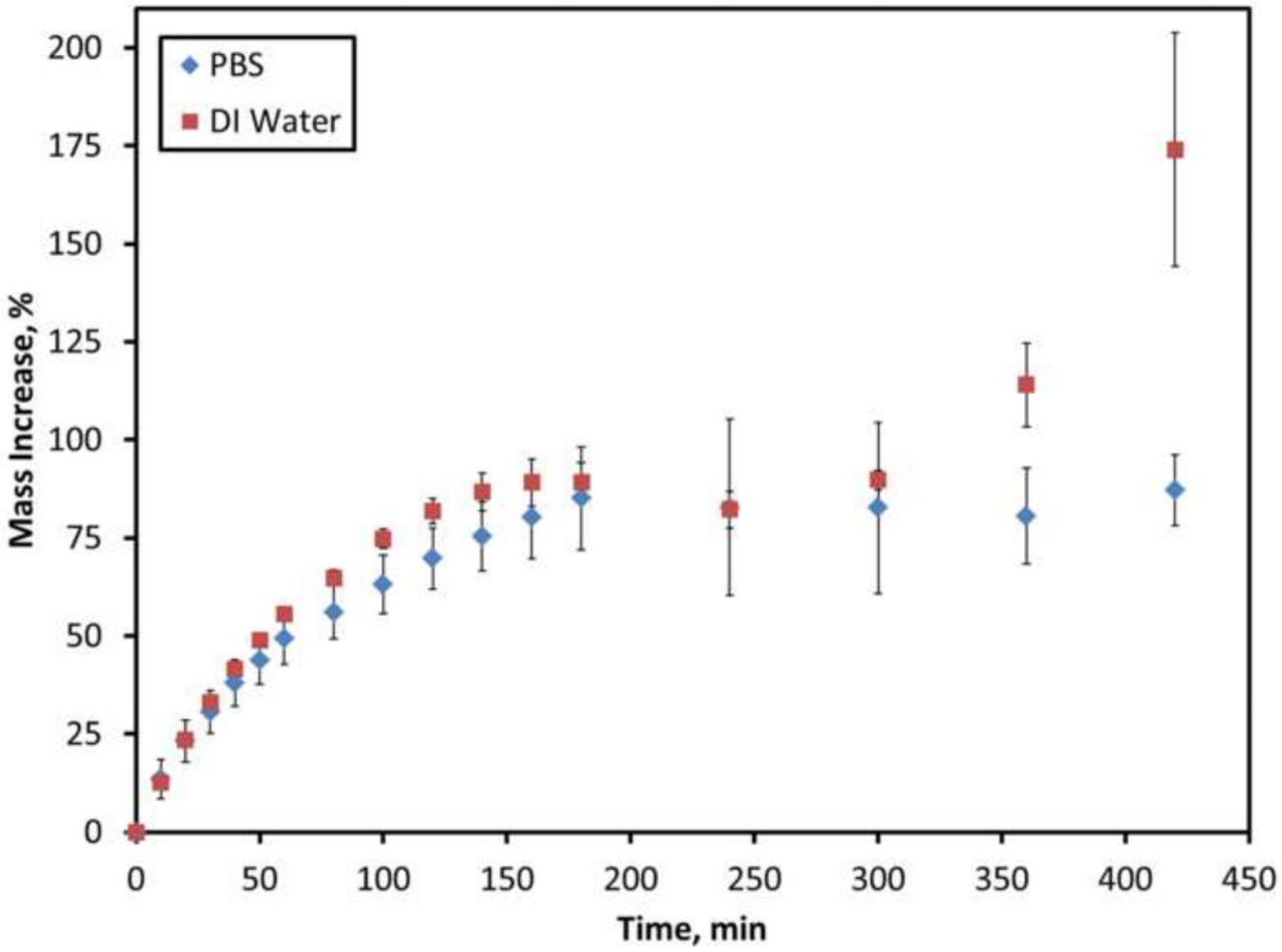

Figure 1.
Swelling of A11 PBAE gels in DI water and PBS. Data are mean ± standard deviation (n=6).

a

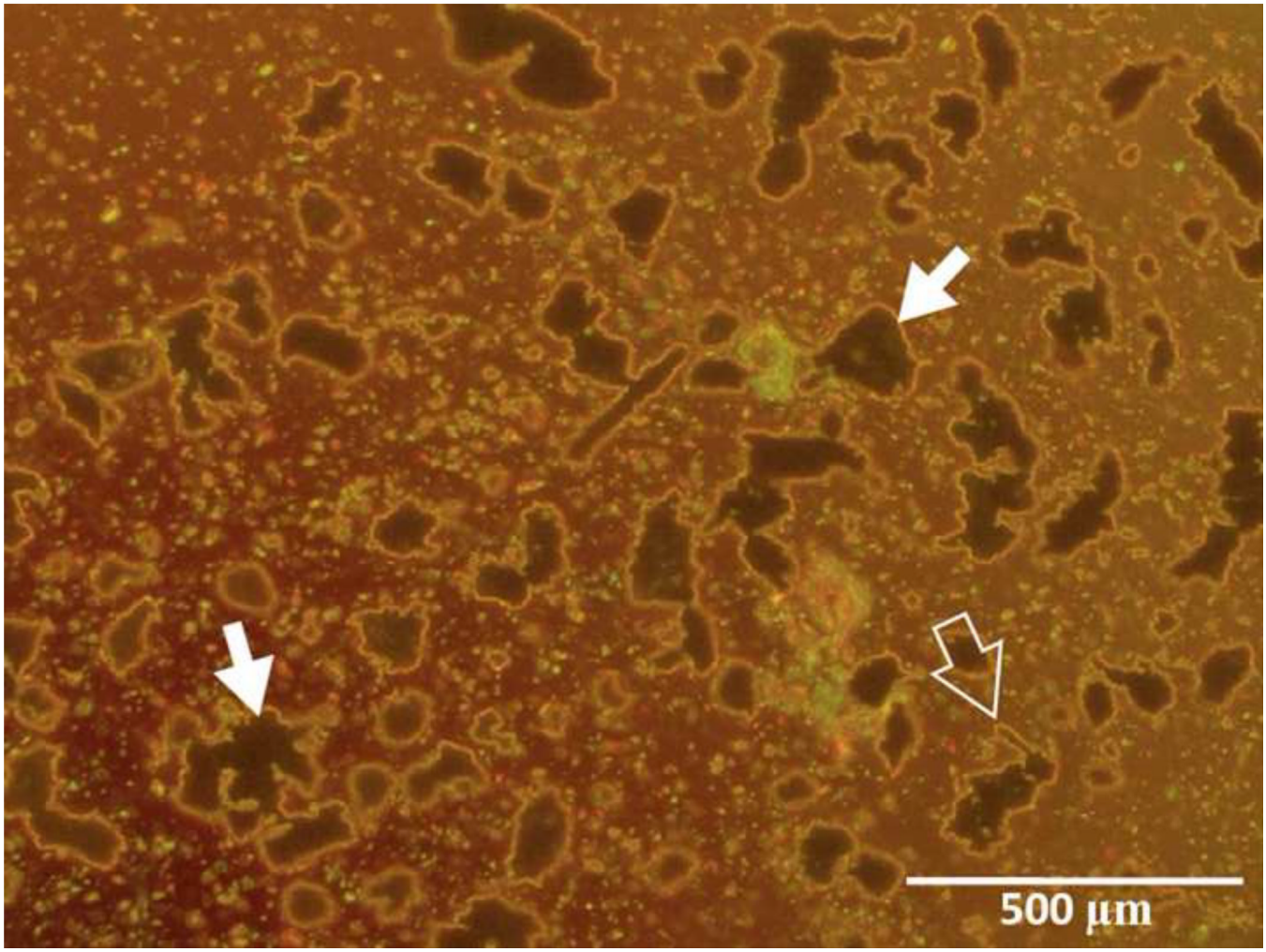

b

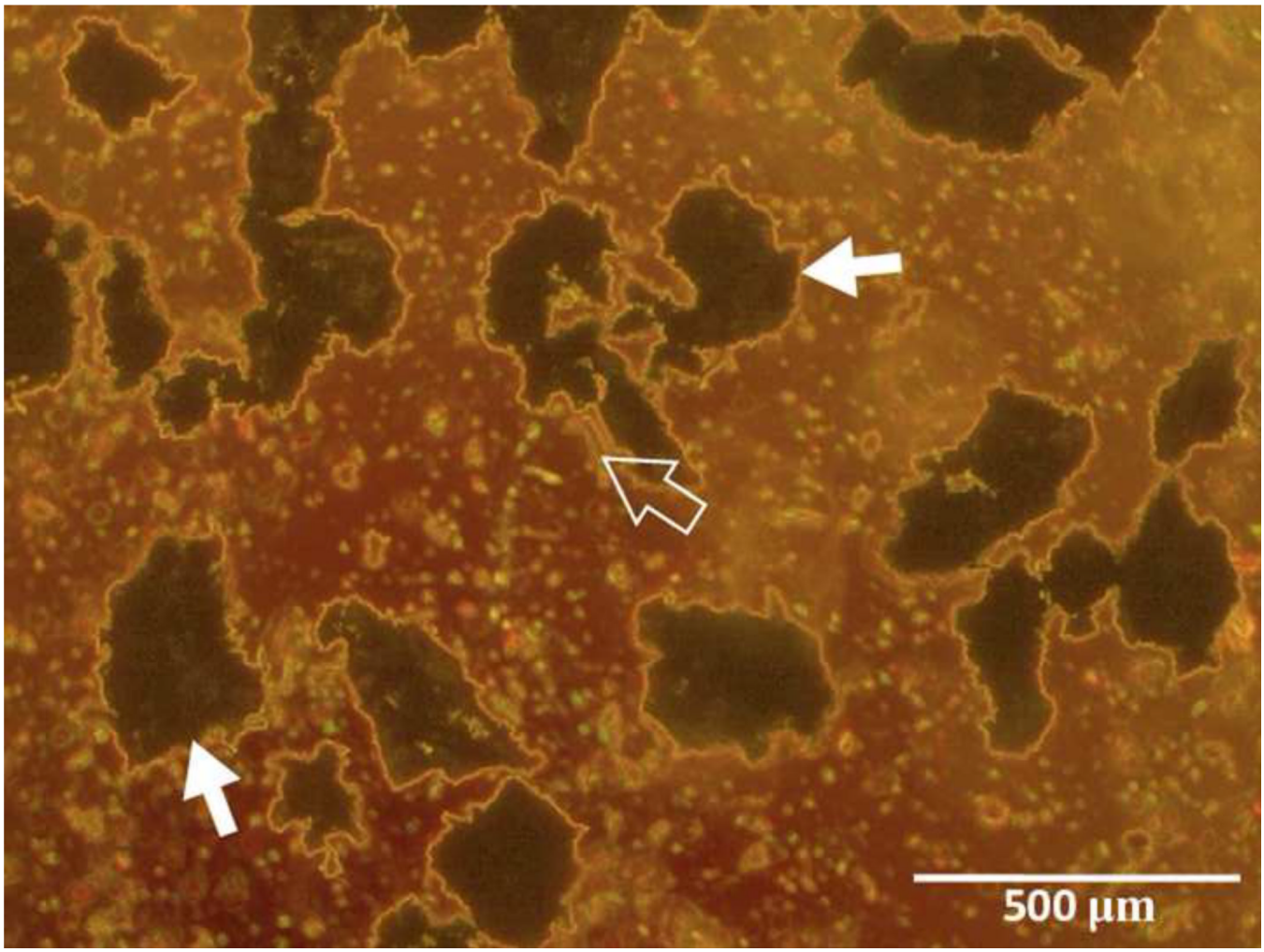

Figure 2.
Morphology of A11 PBAE gel particles: A) 53–150 μm and B) 150–250 μm sieved size fractions. Irregularly shaped objects are gel particles (solid white arrows), and small particles are residual CS (open white arrows).

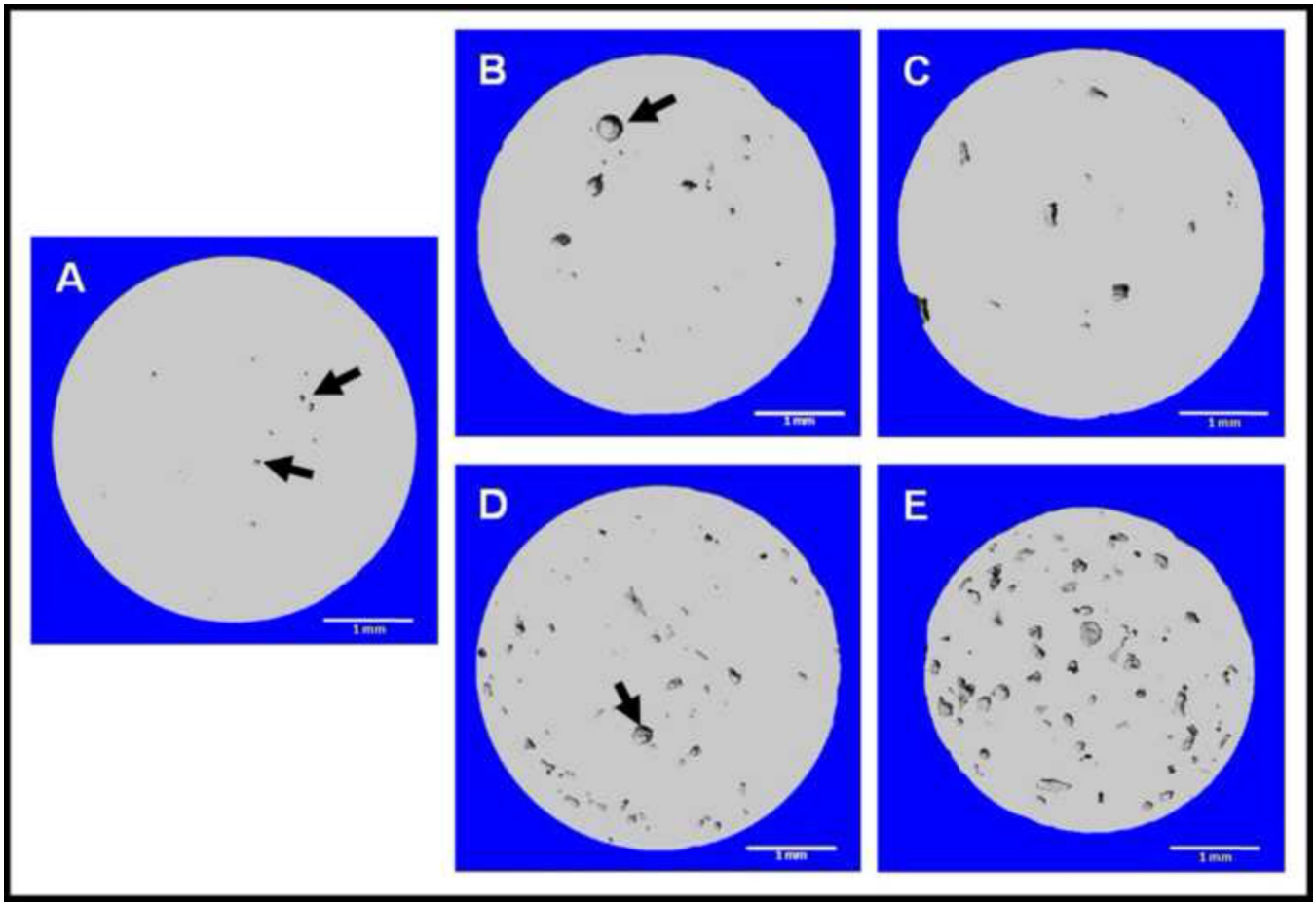

Figure 3.
MicroCT images of CS/HG composites: A) Blank; B) 1 wt% HG, 53–150 μm; C) 1 wt% HG, 150–250 μm; D) 10 wt% HG, 53–150 μm; and E) 10 wt% HG, 150–250 μm. Air pockets indicated by black arrows. All scale bars are 1.0 mm.

a

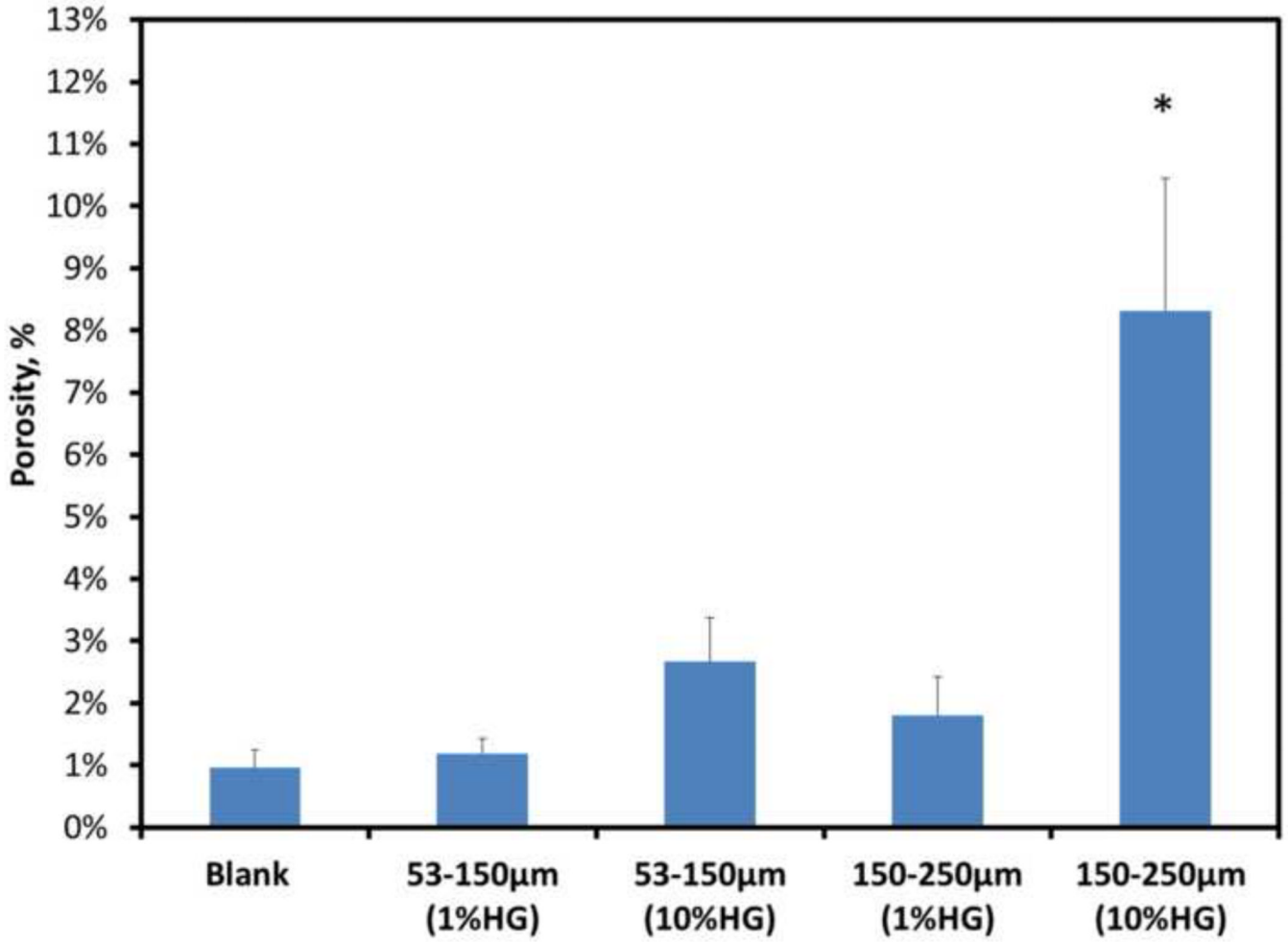

b

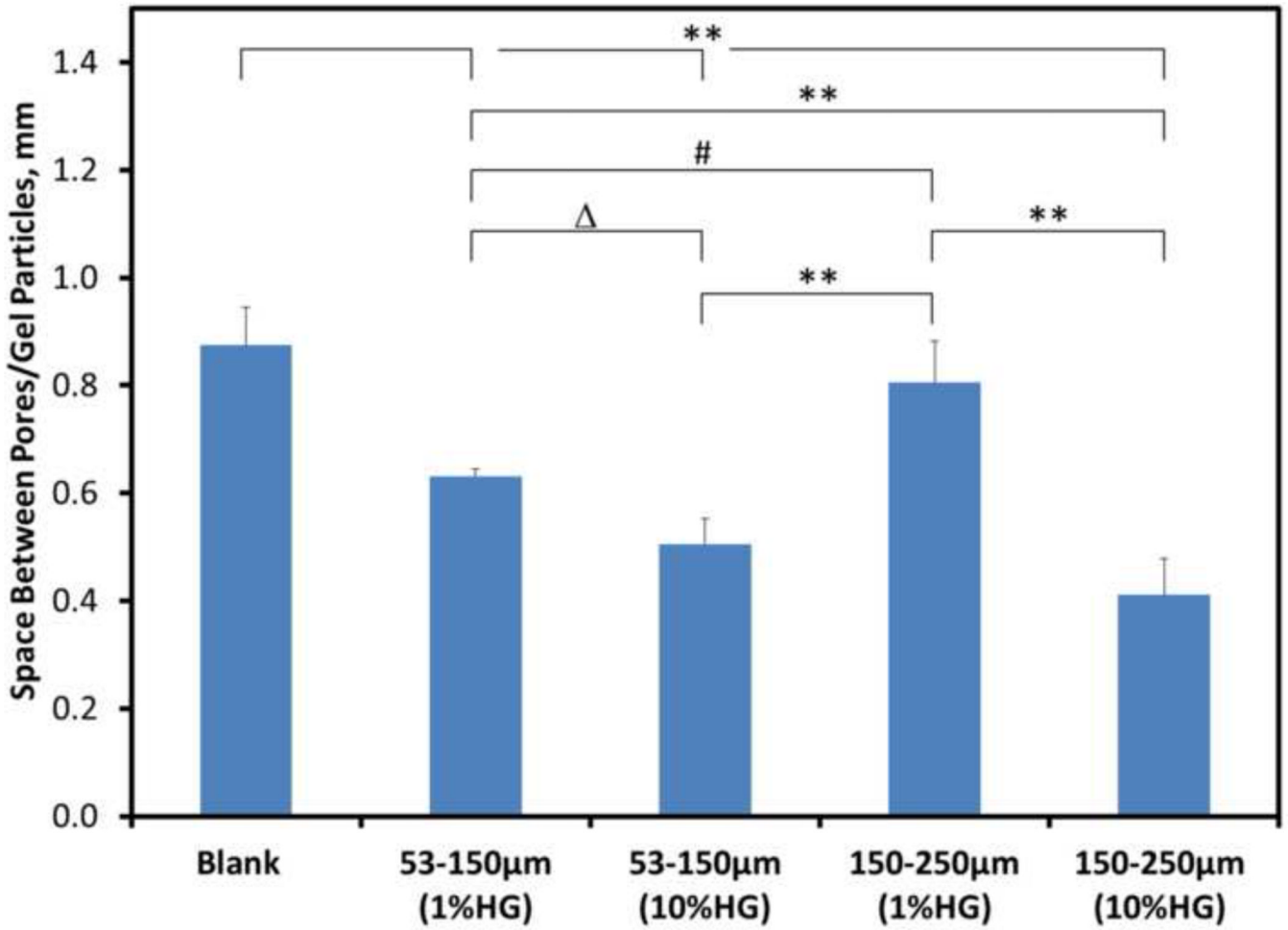

c

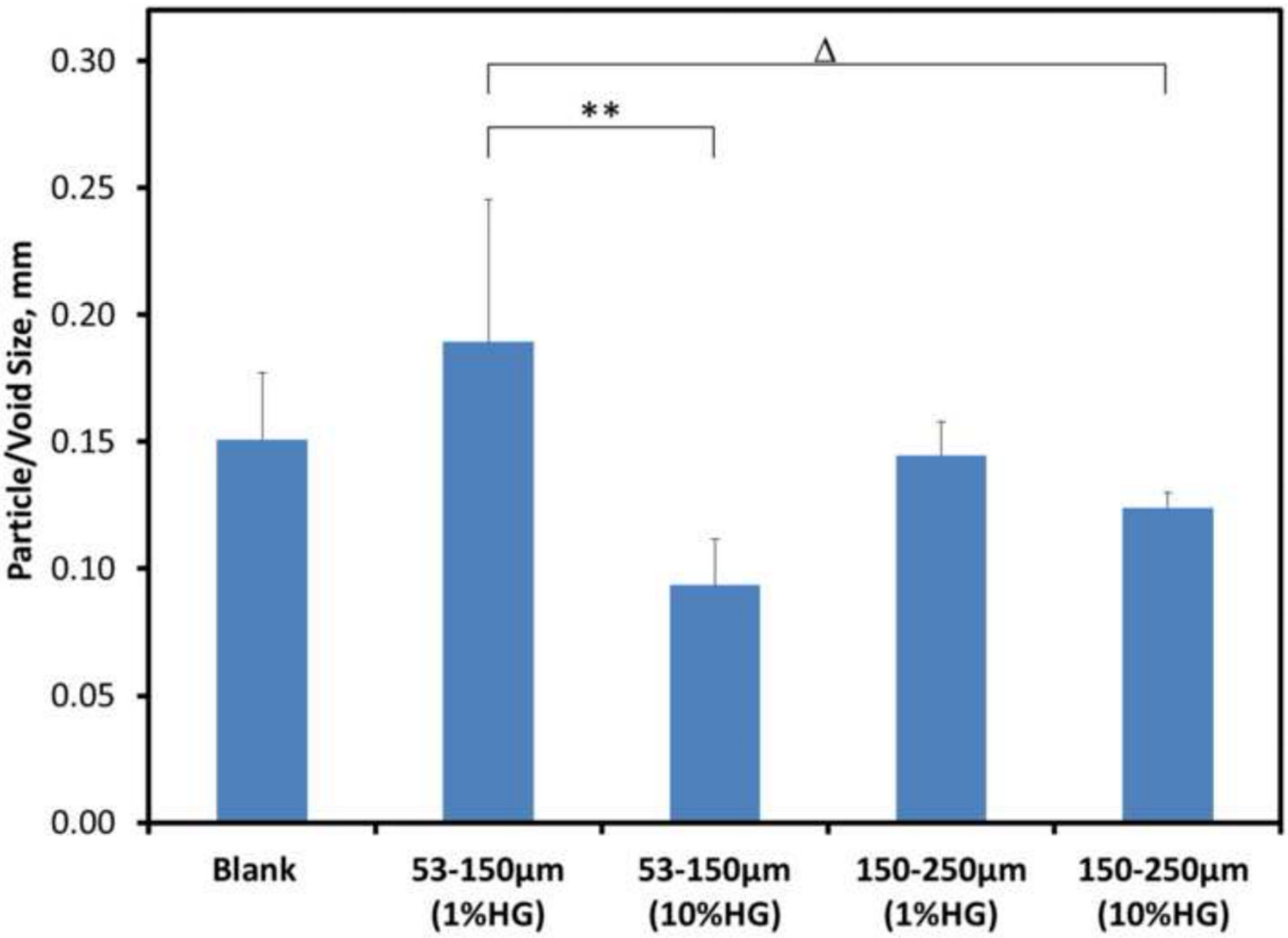

Figure 4.

Quantitative morphometric results from microCT: A) porosity, B) spacing between particles, and C) size of particles/voids within CS matrix for blank and composite samples. Data are mean ± standard deviation (n=5). Bars represent significant differences between a given set of treatments. Symbols indicate the level of significance: $p<0.001$ (*), $p<0.001$ (**), $p<0.01$ (#), and $p<0.05$ (Δ).

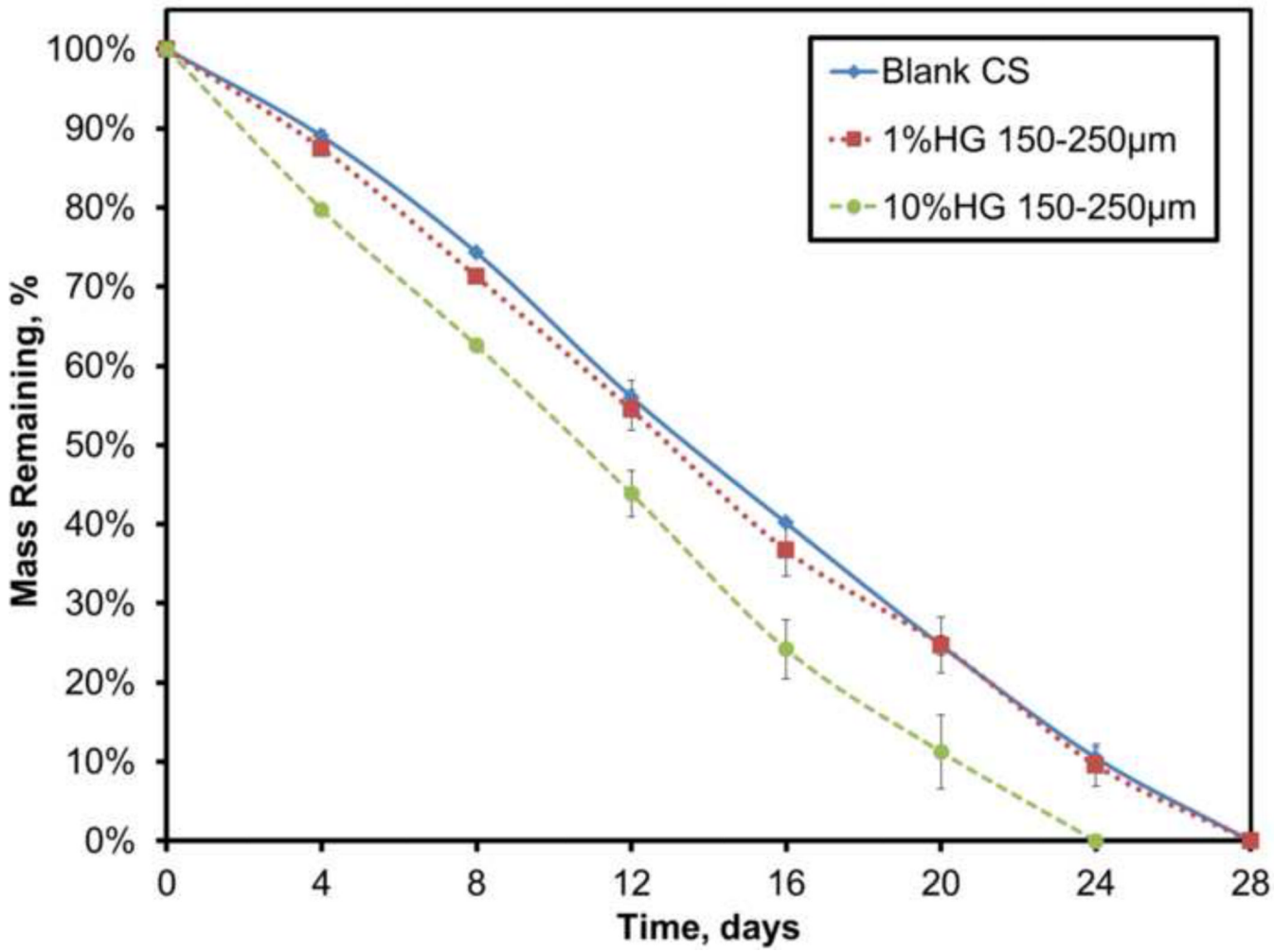

Figure 5.
Dissolution profiles for blank CS and 1 and 10 wt% HG composites. Data are mean ± standard deviation (n=3).

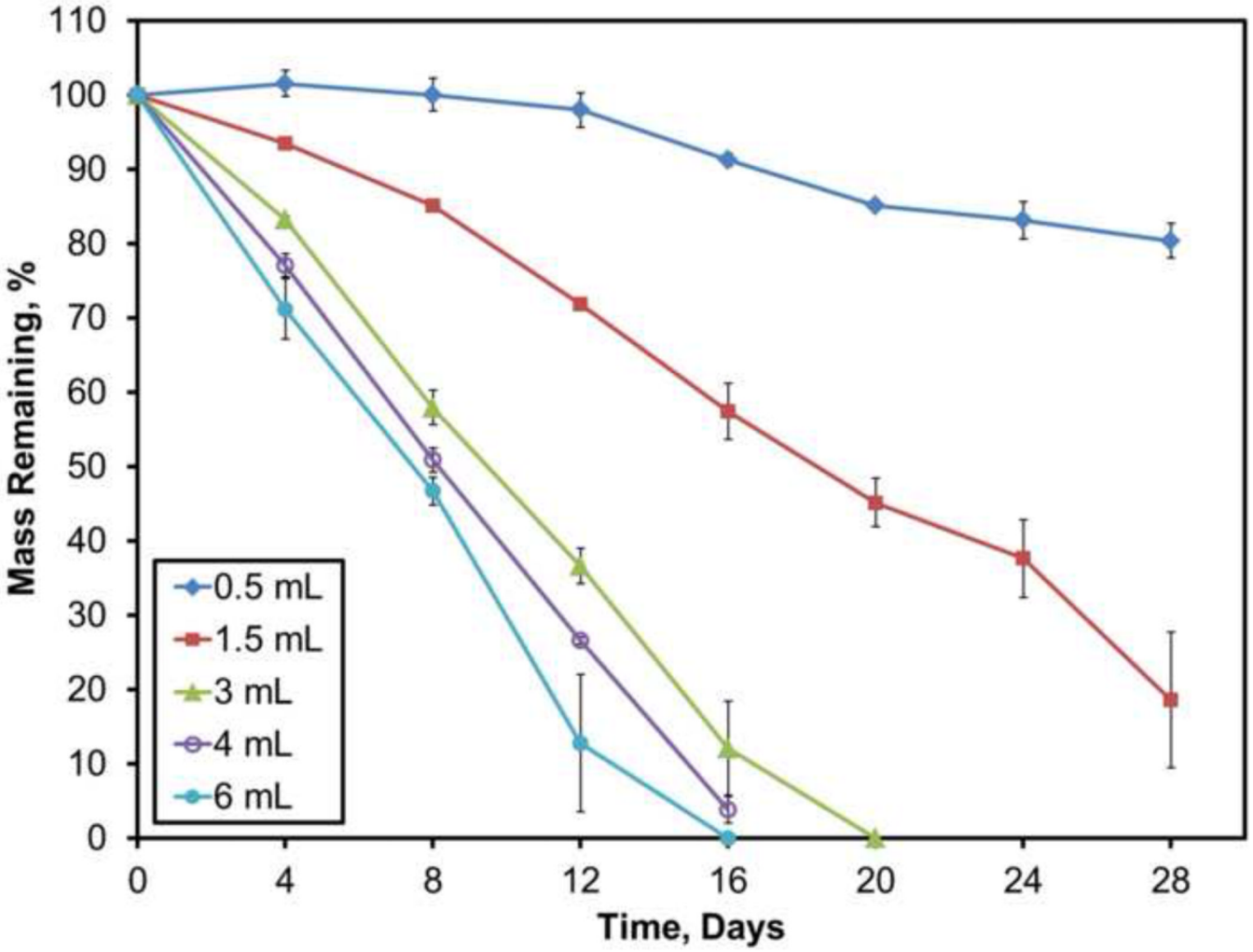

Figure 6.
Dissolution profiles for blank calcium sulfate incubated in different volumes of PBS. Data are mean ± standard deviation (n=3).

a

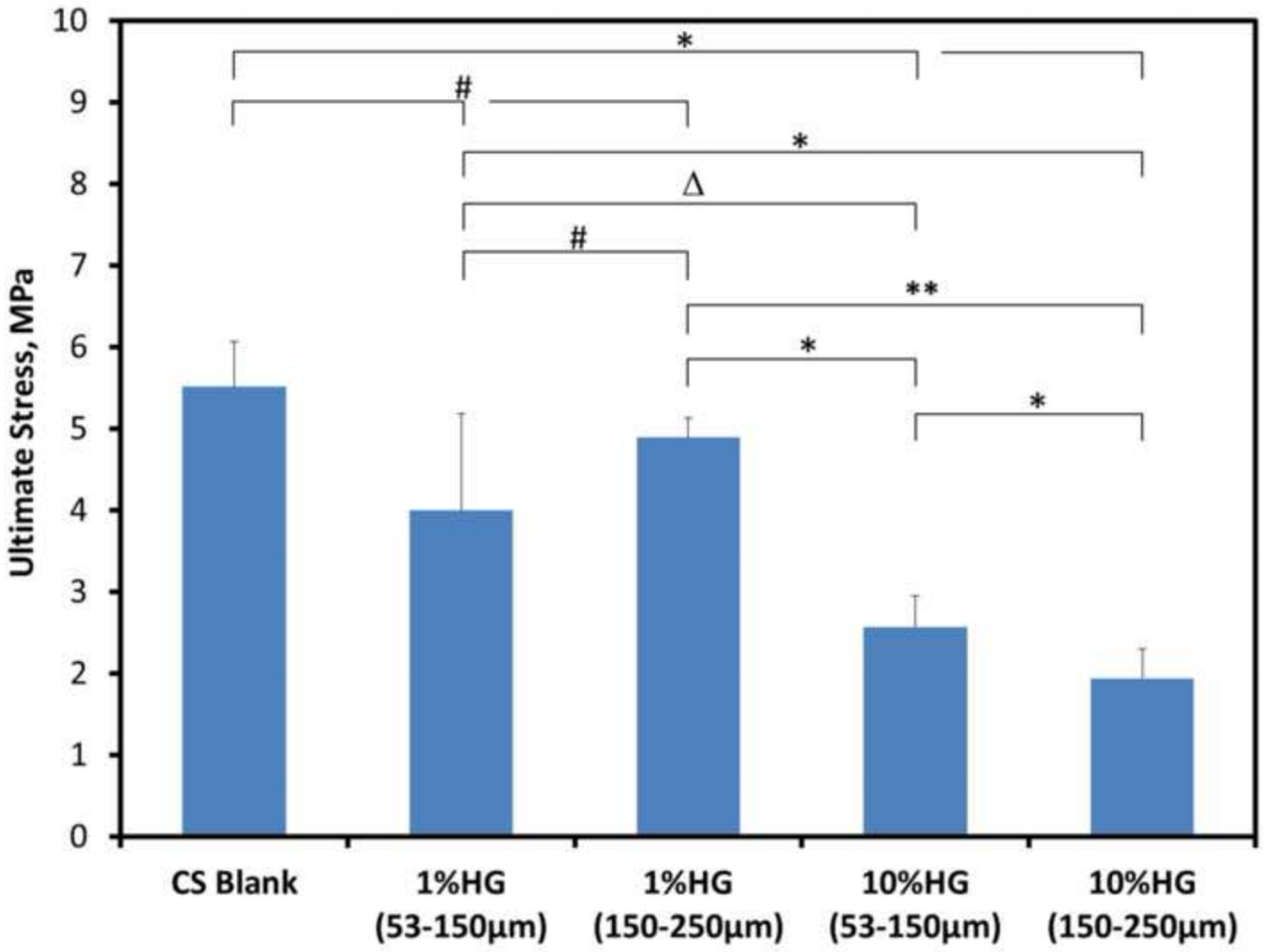

'b

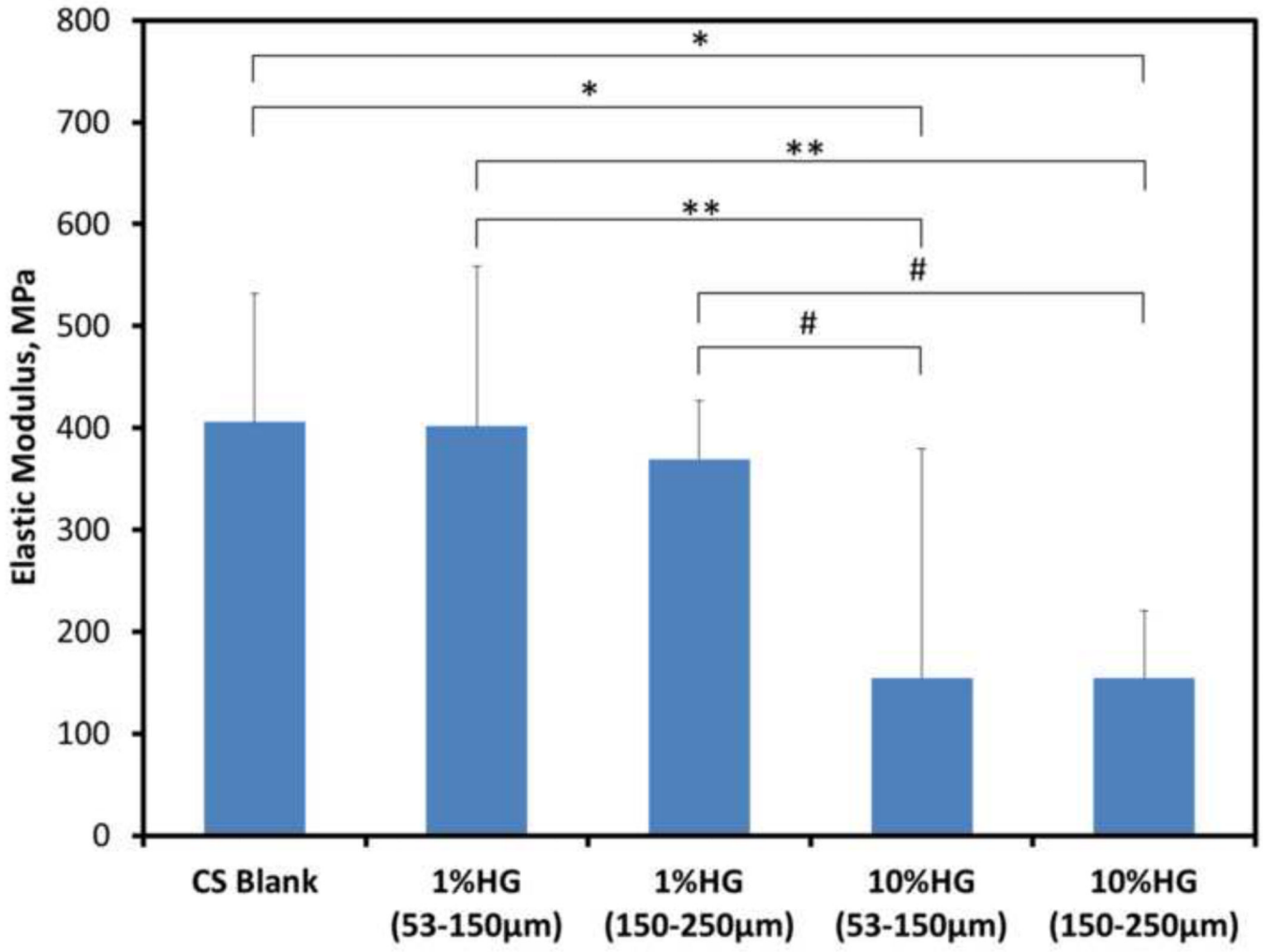

Figure 7.

Mechanical properties of CS/HG composites: A) ultimate compressive strength and B) compressive modulus of blank and composite CS samples. Data are mean ± standard deviation (n=10). Bars represent significant differences between a given set of treatments. Symbols indicate the level of significance: $p<0.0001$ (*), $p<0.001$ (**), $p<0.01$ (#), and $p<0.05(\Delta)$.

a

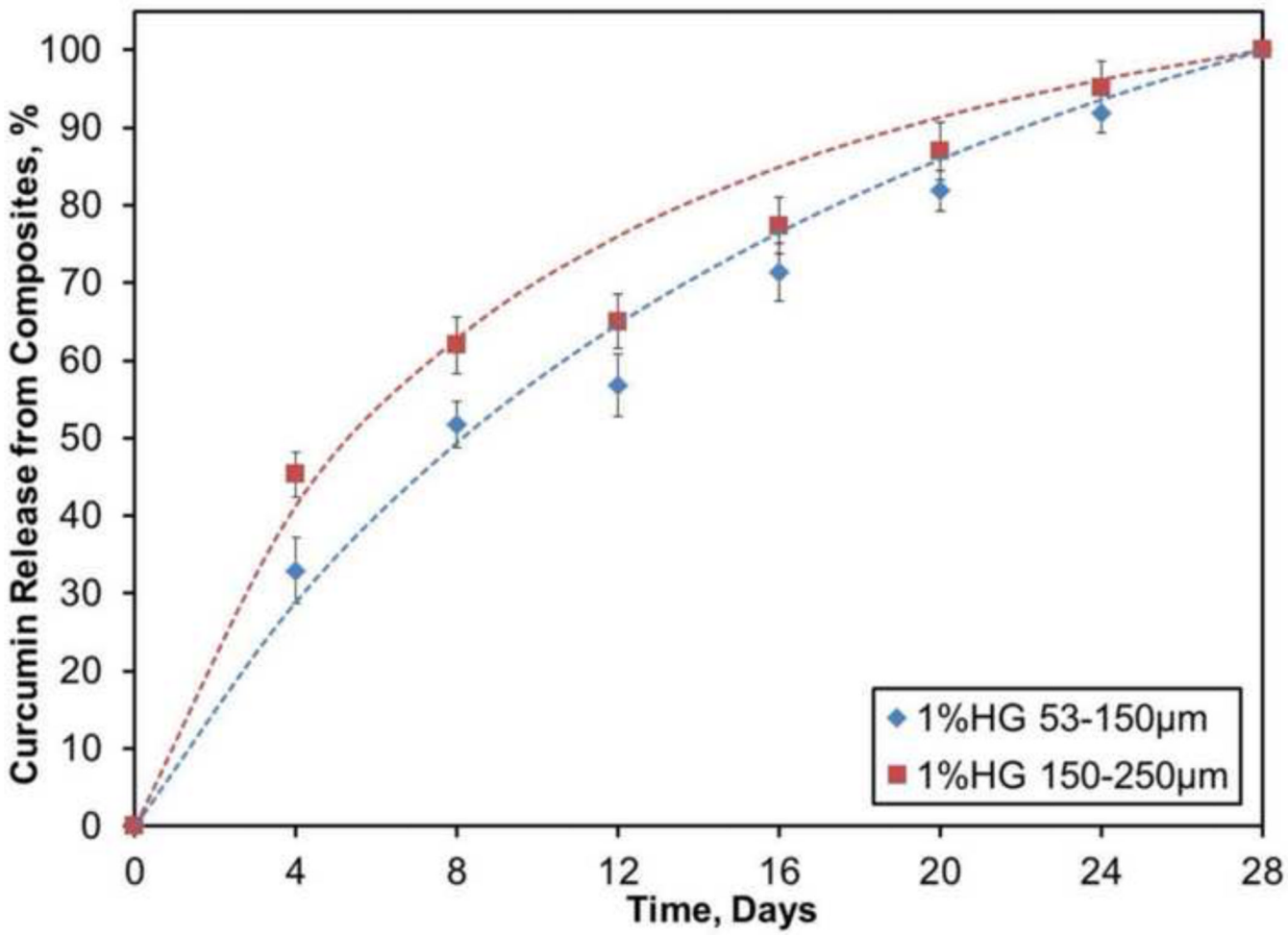

b

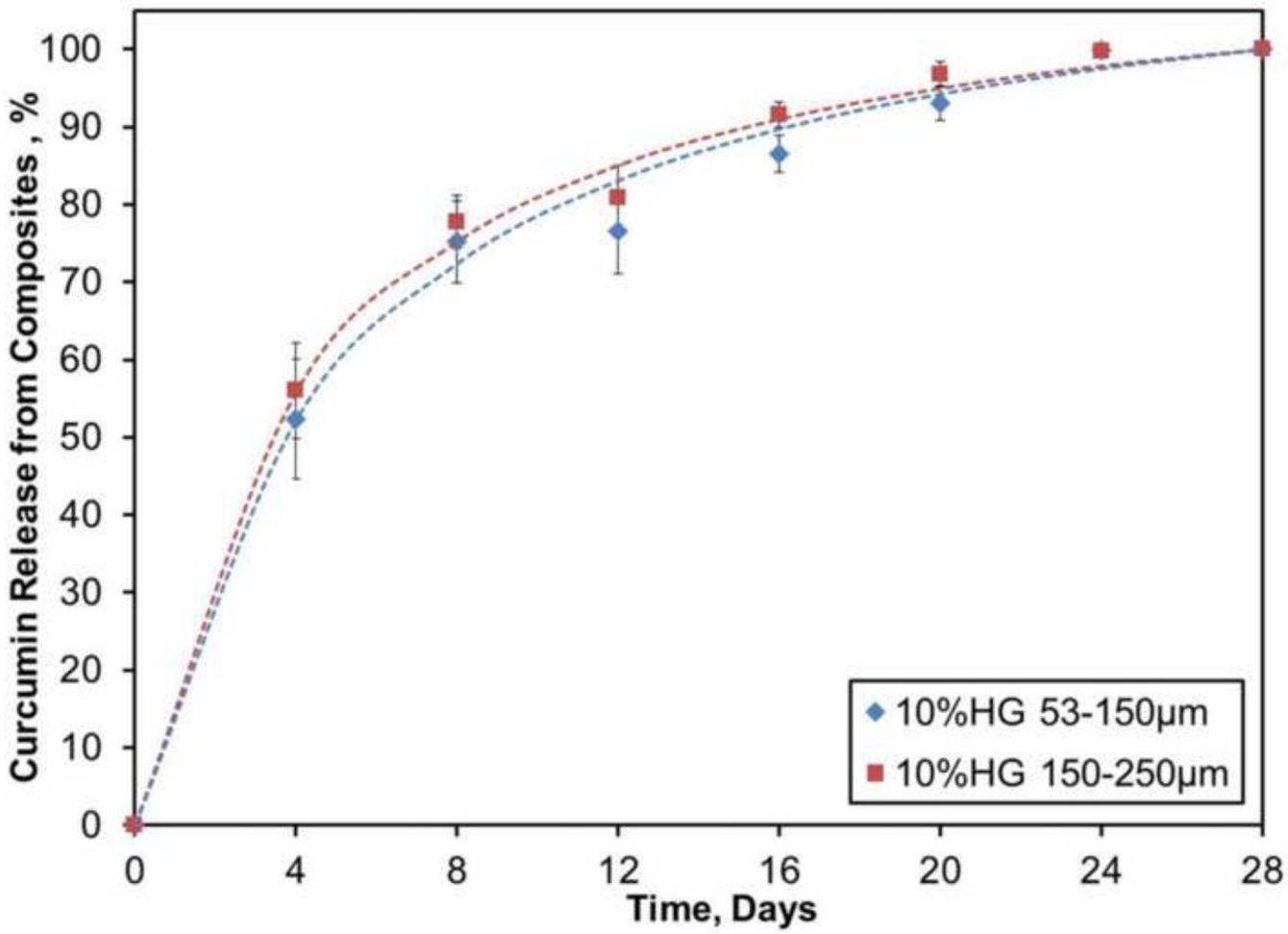

Figure 8.
Profiles showing cumulative release of curcumin from: A) 1 wt% HG and B) 10 wt% HG composites. Data are mean ± standard deviation (n=5).